

Supplementary Information

Solid Additive Tuning Polymer Blend Morphology Enables Non-halogenated-solvent All-polymer Solar Cells with an Efficiency over 17%

Ke Hu,^{‡a,b} Can Zhu,^{‡a,b} Kan Ding,^c Shucheng Qin,^{a,b} Wenbin Lai,^{a,b} Jiaqi Du,^{a,b} Jianqi Zhang,^d Zhixiang Wei,^d Xiaojun Li,^b Zhanjun Zhang,^{*a} Lei Meng,^{*a,b} Harald Ade,^{*c} and Yongfang Li,^{*a,b,e}

^a School of Chemical Science, University of Chinese Academy of Sciences, Beijing 100049, China

^b Beijing National Laboratory for Molecular Sciences, CAS Key Laboratory of Organic Solids, Institute of Chemistry, Chinese Academy of Sciences, Beijing 100190, China

^c Department of Physics and Organic and Carbon Electronics Laboratories (ORaCEL), North Carolina State University, Raleigh, NC, USA.

^d CAS key laboratory of nanosystem and hierarchical fabrication, CAS Center for Excellence in Nanoscience, National Center for Nanoscience and Technology, 100190 Beijing, China

^e Laboratory of Advanced Optoelectronic Materials, Suzhou Key Laboratory of Novel Semiconductor-optoelectronics Materials and Devices, College of Chemistry, Chemical Engineering and Materials Science, Soochow University, Suzhou, Jiangsu 215123, China

[‡] K. Hu and C. Zhu contribute equally to this work.

***Corresponding authors:** zhangzj@ucas.ac.cn (Z. Zhang), menglei@iccas.ac.cn (L. Meng), hwade@ncsu.edu (H. Ade), liyf@iccas.ac.cn (Y. Li).

Experimental Section

The polymer PBQ6 was provided by our laboratory. Polymer PYF-T-*o* was purchased from eFlexPv. All the solvents and chemicals were obtained commercially and used without further purification, unless otherwise stated. The pre-patterned ITO glass is purchased from Advanced Election Technology Co., Ltd.

Characterization of materials

Gel permeation chromatography (GPC) measurement was performed on Agilent PL-GPC 220 instrument with high temperature chromatograph, using 1,2,4-trichlorobenzene as the eluent at 160 °C. UV-Vis absorption spectra were recorded on Hitachi U-3010 UV-vis spectrophotometer. For the film measurements, PBQ6 and PYF-T-*o* films were prepared by spin-coating their solutions in chloroform on quartz plates.

Cyclic voltammetry measurement was performed on the Zahner IM6e electrochemical workstation, using a glassy carbon electrode as the working electrode, platinum wire as the counter electrode and Ag/AgCl as the reference electrode, at a potential scanning rate of 50 mV·s⁻¹ in 0.1 M tetrabutylammonium hexafluorophosphate (Bu₄NPF₆) acetonitrile solution. The ferrocene/ferrocene (Fc/Fc⁺) pair was used as an internal reference. **The $E_{\text{HOMO}}/E_{\text{LUMO}}$ values were calculated from the onset oxidation/reduction potentials ($\phi_{\text{ox}}/\phi_{\text{red}}$) obtained from the cyclic voltammograms, according to the equations of $E_{\text{HOMO}}/E_{\text{LUMO}} = -e (\phi_{\text{ox}}/\phi_{\text{red}} + 4.8 - \phi_{\text{Fc}/\text{Fc}^+})$ (eV), where redox potentials of $\phi_{\text{Fc}/\text{Fc}^+}$ was measured to be 0.47 V versus Ag/AgCl.**

Device fabrication and characterization

The all-polymer solar cells (all-PSCs) were fabricated with a structure of ITO/PEDOT:PSS (40 nm)/active layer/PDINN/Ag. The ITO-coated glass substrates were cleaned by ultrasonic treatment in deionized water, acetone, and isopropanol for 15 min, dried under a nitrogen stream, and subsequent ultraviolet-ozone treatment for 20 min. A thin layer of PEDOT:PSS was deposited on precleaned ITO-coated glass through spin-coating PEDOT:PSS aqueous solution (Baytron P VP AI 4083 from H.C.

Starck) at 6000 rpm and dried subsequently at 150 °C for 15 min in air, then the PEDOT:PSS-coated ITO glass electrode was transferred to a nitrogen glove box. The blend solutions of PBQ6:PYF-T-*o* (1:1, wt/wt) were prepared in toluene (the total concentration of blend solutions was 16 mg mL⁻¹), with the addition of chloronaphthalene (CN) or dithieno[3,2*b*:2',3'-*d*]thiophene (DTT) as additive. The solutions were stirred and heated at 50 °C. The blend solutions were spin-cast onto the PEDOT:PSS layer at a spin-coating rate of 2500 rpm. After the active layers were treated with thermal annealing at 90°C for 10 min, the methanol solution of PDINN with a concentration of 1.0 mg mL⁻¹ was spin-coated atop the active layer at 3000 rpm for 30 s to form a PDINN cathode buffer layer with thickness of ca. 10 nm. Finally, top Ag electrode was deposited in vacuum onto the cathode buffer layer at a pressure of ca. 1.0 × 10⁻⁶ Pa. The active area of the PSCs was 6.0 mm², which was defined by Optical microscope (Olympus BX51).

For devices fabricated in air, the ITO-coated glass substrates were cleaned by ultrasonic treatment in deionized water, acetone, and isopropanol for 15 min, dried under a nitrogen stream, and subsequent ultraviolet-ozone treatment for 20 min. A thin layer of PEDOT:PSS was deposited on precleaned ITO-coated glass through spin-coating PEDOT:PSS aqueous solution at 6000 rpm and dried subsequently at 150 °C for 15 min in air, then the PEDOT:PSS-coated ITO glass electrode was transferred to a fume hood. The blend solutions of PBQ6:PYF-T-*o* (1:1, w/w) were prepared in toluene (the total concentration of blend solutions was 16 mg mL⁻¹), with the addition of chloronaphthalene (CN) or dithieno[3,2*b*:2',3'-*d*]thiophene (DTT) as additive. The solutions were stirred and heated at 50 °C. The blend solutions were spin-cast onto the PEDOT:PSS layer at a spin-coating rate of 2500 rpm with a relative humidity of 30% and an ambient temperature of 27 °C. The active layers were treated with thermal annealing at 90°C for 10 min, and then transferred to a nitrogen glove box. The methanol solution of PDINN with a concentration of 1.0 mg mL⁻¹ was spin-coated atop the active layer at 3000 rpm for 30 s to form a PDINN cathode buffer layer with thickness of ca. 10 nm. Finally, top Ag electrode was deposited in vacuum onto the

cathode buffer layer at a pressure of ca. 1.0×10^{-6} Pa. The active area of the PSCs was 6.0 mm^2 , which was defined by Optical microscope (Olympus BX51).

The current density–voltage (J – V) characteristics of the all-PSCs were measured in a nitrogen glove box with a Keithley 2450 Source Measure unit. Oriel Sol3A Class AAA Solar Simulator (model, Newport 94023A) with a 450W xenon lamp and an air mass (AM) 1.5 filter was used as the light source. The light intensity was calibrated to 100 mW cm^{-2} by a Newport Oriel 91150V reference cell. The input photon to converted current efficiency (IPCE) was measured by Solar Cell Spectral Response Measurement System QE-R3-011 (Enli Technology Co., Ltd., Taiwan). The light intensity at each wavelength was calibrated with a standard single-crystal Si photovoltaic cell.

In the Photo-CLIVE, and TPV measurements, the PSCs were fabricated with the same method as mentioned above. The data were obtained by the all-in-one characterization platform, Paios (Fluxim AG, Switzerland). In the photo-CELIV measurement, the delay time is set to 0 s, the light intensity is 100%, the light-pulse length is $100 \mu\text{s}$, finally the sweep ramp rate rises from 20 V/ms to 100 V/ms. In the TPV measurement, the light intensity is 0.10%, 0.23%, 0.53%, 1.23%, 2.83%, 6.52%, 15.0%, 34.6% and 80.0%, respectively, relative intensity is 20.0% and settling time is 30.0 ms, pulse length is 5.0 ms and the follow-up time is $30.0 \mu\text{s}$.

Mobility measurements.

The charge carrier mobilities were measured with the device structure of ITO/PEDOT:PSS/active layer/ MoO_3 /Ag for hole-mobility and ITO/ZnO/active layer/PDINN/Ag for electron-mobility. The hole and electron mobilities were calculated according to the space charge limited current (SCLC) method equation: $J = 9\mu\epsilon_r\epsilon_0 V^2/8d^3$, where J is the current density, μ is the hole or electron mobility, V is the internal voltage in the device, ϵ_r is the relative dielectric constant of active layer material, ϵ_0 is the permittivity of empty space, and d is the thickness of the active layer.

Atomic force microscopy (AFM) and Transmission electron microscopy (TEM)

The morphologies of the polymer/acceptor blend films were investigated by AFM (Bruker multimode8 AFM) in contacting under normal air conditions at room

temperature with a 5 μm scanner. Samples for the TEM measurements were prepared as following: The active layer films were spin-casted on ITO/poly (3,4-ethylenedioxythiophene) poly (styrenesulfonate) (PEDOT:PSS) substrates, and the substrates with active layers were submerged in deionized water to make the active layers floats onto the air-water interface. Then, the floated films were picked up on an unsupported 200 mesh copper grids for the TEM measurements. TEM experiments were performed on a JEM-2100 transmission electron microscope operated at 200 kV.

GIWAXS measurements

Grazing-incidence wide-angle X-ray scattering (GIWAXS) measurements GIWAXS measurements were performed on a XEUSS SAXS/WAXS system (XENOCs, France) at the National Center for Nanoscience and Technology (NCNST, Beijing).

Resonant soft X-ray scattering (RSoXS)

Resonant soft X-ray scattering was performed at beamline 11.0.1.2 Advanced Light Source, LBNL. Thin film samples were spin-casted on top of the PEDOT:PSS covered Si wafers under exactly the same condition as those for the fabrication of solar cell devices. Then BHJ thin films were floated and transferred onto silicon nitride membrane windows. The scattering was done in transmission mode and signals were collected in vacuum using Princeton Instrument PI-MTE CCD camera. The RSoXS profiles are Lorentz corrected and thickness normalized.

Supplementary Figures

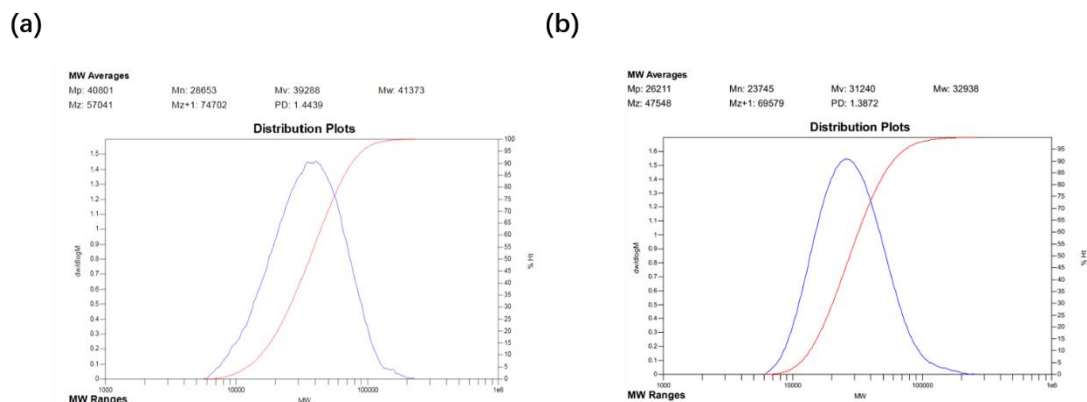


Figure S1. GPC results of PBQ6 and PYF-T-*o*.

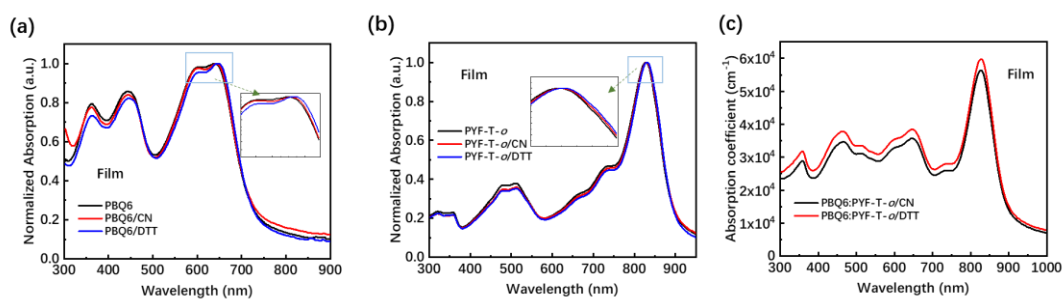


Figure S2. Absorption spectra of (a) PBQ6 and (b) PYF-T-*o* film processed by different additive treatment. (c) UV-vis absorption spectra of PBQ6:PYF-T-*o* films with CN or DTT.

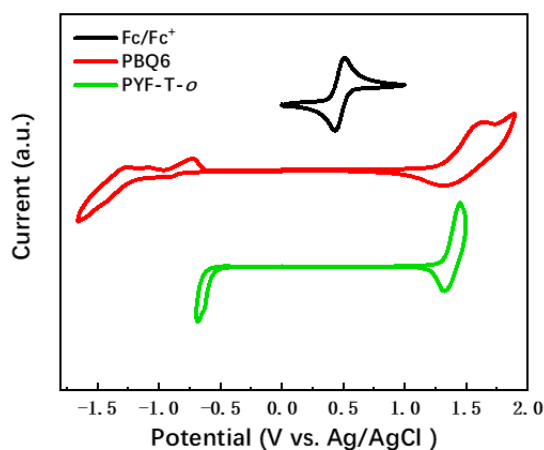


Figure S3. Cyclic voltammograms of PBQ6 and PYF-T-*o* measured in acetonitrile solutions of $0.1 \text{ mol L}^{-1} n\text{-Bu}_4\text{NPF}_6$ using ferrocene (Fc/Fc^+) as an internal reference.

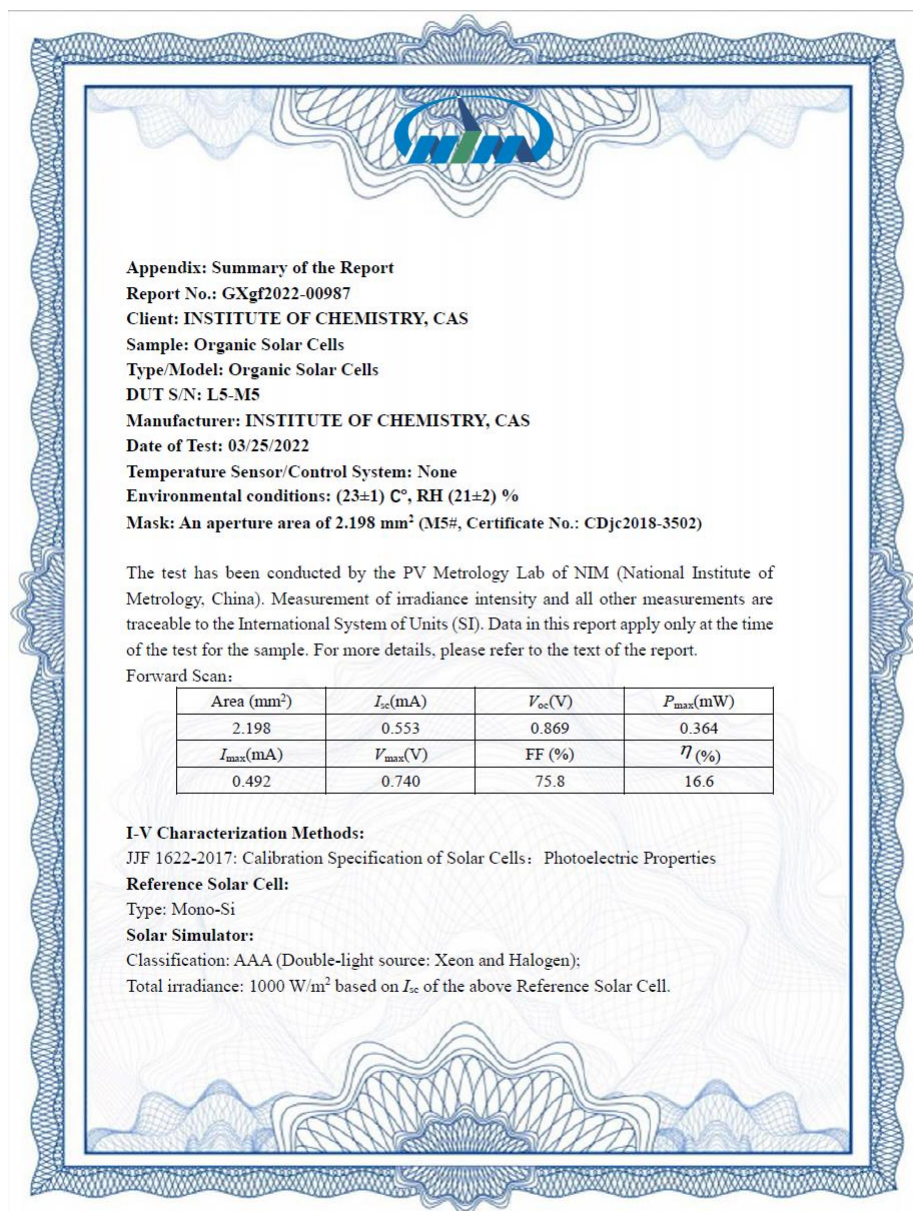


Figure S4. The certified photovoltaic performance of the all-PSC based on PBQ6:PYF-T-o film with DTT solid additive treatment, from NIM, China.

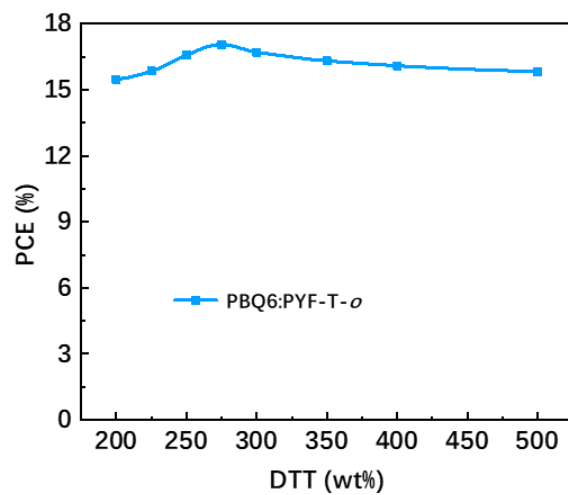


Figure S5. The PCEs for the PBQ6:PYF-T-*o*-based devices with different weight ratio of DTT solid additive treatment.

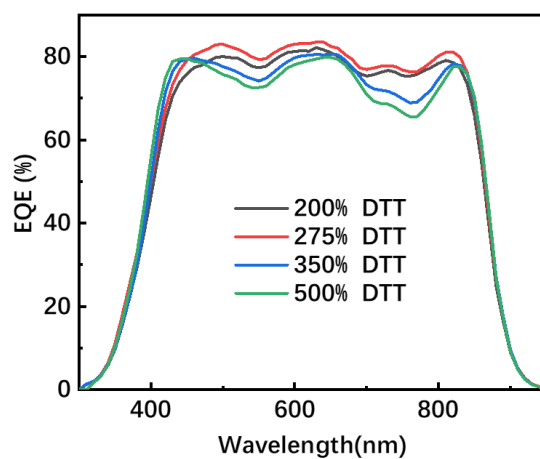


Figure S6. EQE spectra of the devices with different amounts of DTT solid additive treatment.

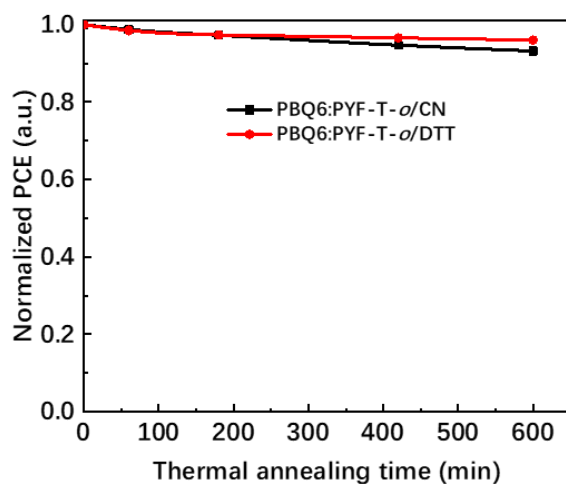


Figure S7. Average normalized PCE of all-PSCs under 150 °C stress for different duration times.

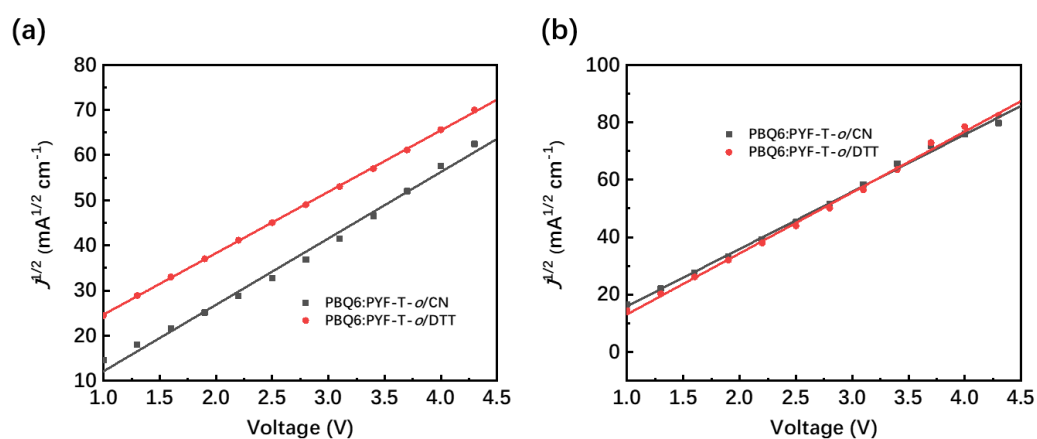


Figure S8. $J^{1/2}$ - V curves of the (a) electron-only devices and (b) hole-only devices for the measurements of charge carriers mobilities.

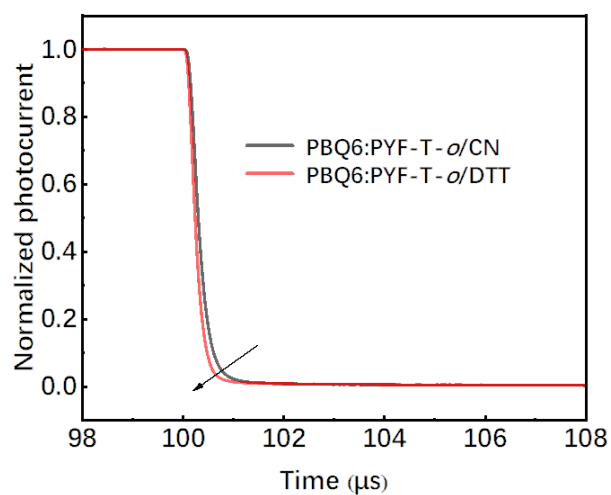


Figure S9. Decay curves of the photocurrent in the transient photocurrent test with time.

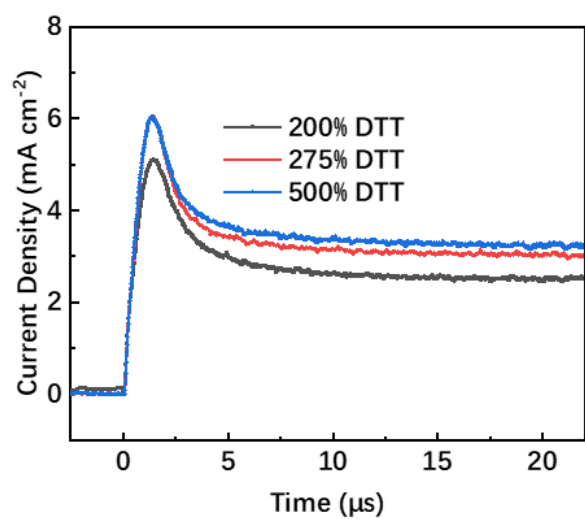


Figure S10. Photo-CELIV characteristics of the all-PSCs with different amounts of DTT solid additive treatment.

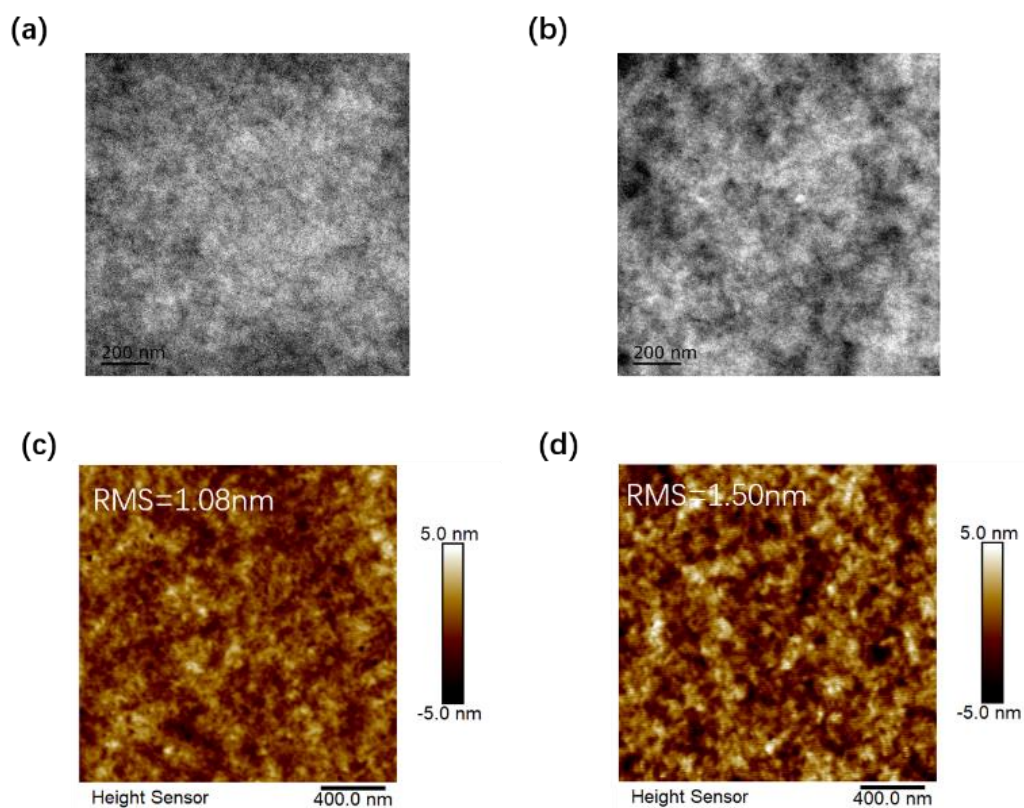


Figure S11. TEM phase images of (a) PBQ6:PYF-T-*o*/CN and (b) PBQ6:PYF-T-*o*/DTT based films. AFM phase images of (c) PBQ6:PYF-T-*o*/CN and (d) PBQ6:PYF-T-*o*/DTT based films.

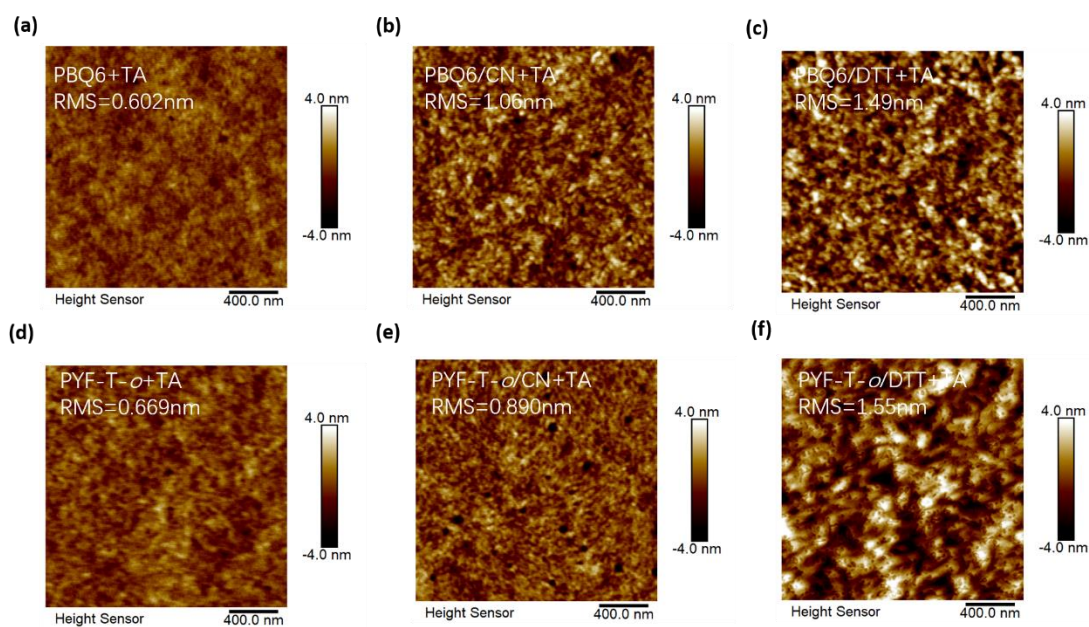


Figure S12. AFM surface scans of (a) PBQ6 and (b) PYF-T-*o* based films with different additives.

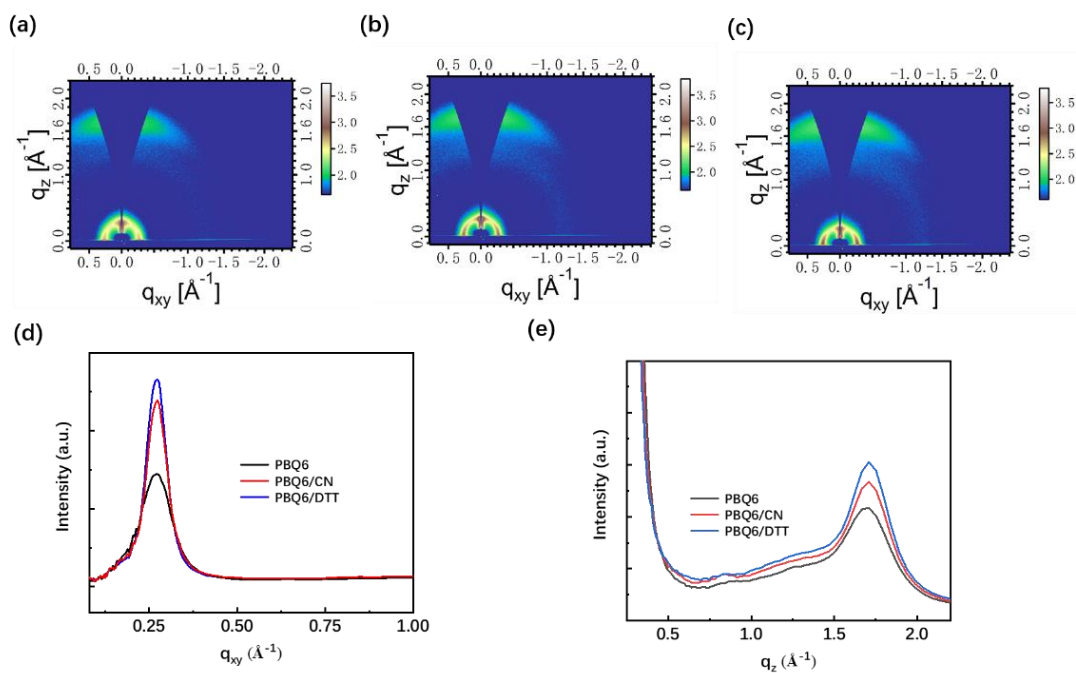


Figure S13. 2D GIWAXS diffraction patterns of (a) PBQ6, (b) PBQ6/CN and (c) PBQ6/DTT. (d) IP and (e) OOP line-cut profiles of GIWAXS images with the corresponding conditions.

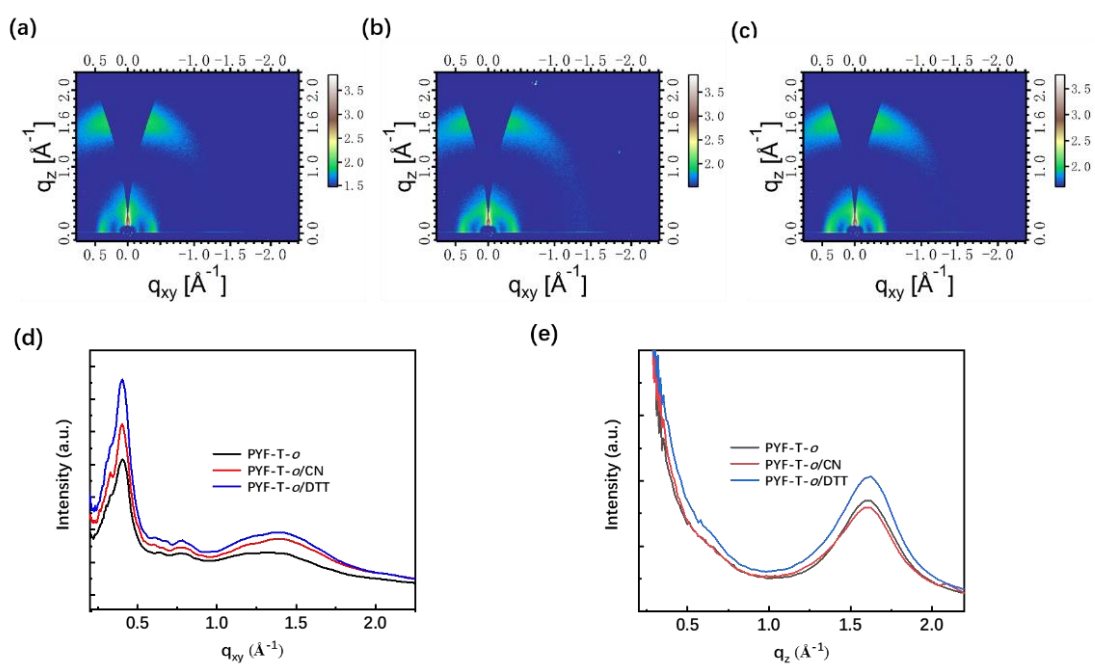


Figure S14. 2D GIWAXS diffraction patterns of (a) PYF-T-*o*, (b) PYF-T-*o*/CN and (c) PYF-T-*o*/DTT. (d) IP and (e) OOP line-cut profiles of GIWAXS images with the corresponding conditions.

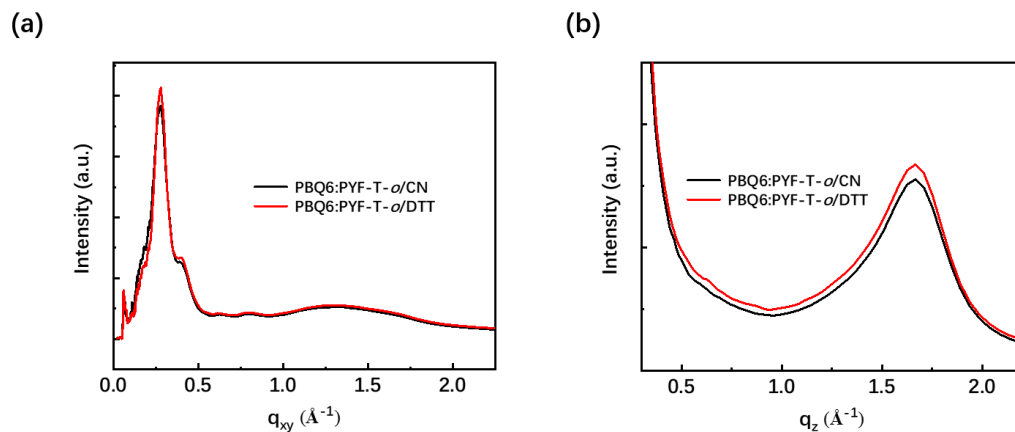


Figure S15. (a) IP and (b) OOP line-cut profiles of GIWAXS images with PBQ6:PYF-T-*o*/CN and PBQ6:PYF-T-*o*/DTT.

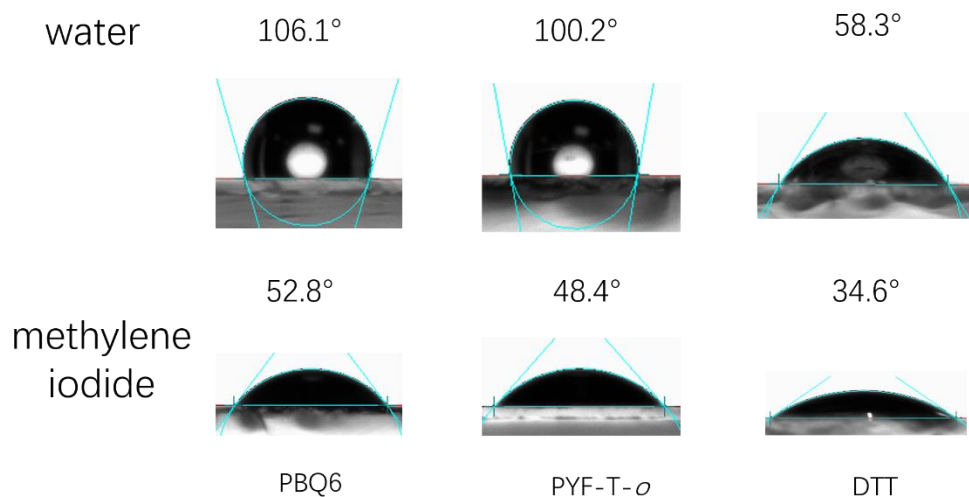


Figure S16. Contact angles of PBQ6, PYF-T-*o* and DTT.

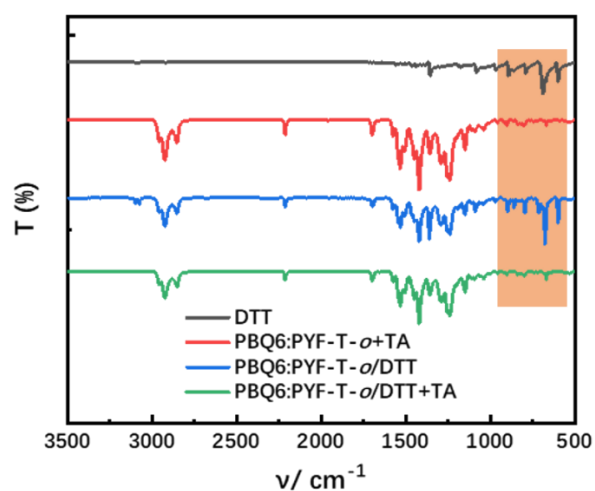


Figure S17. FTIR spectra of DTT, PBQ6:PYF-T-*o*, PBQ6:PYF-T-*o*/DTT and PBQ6:PYF-T-*o*/DTT with the TA treatment at 90 °C for 10 min.

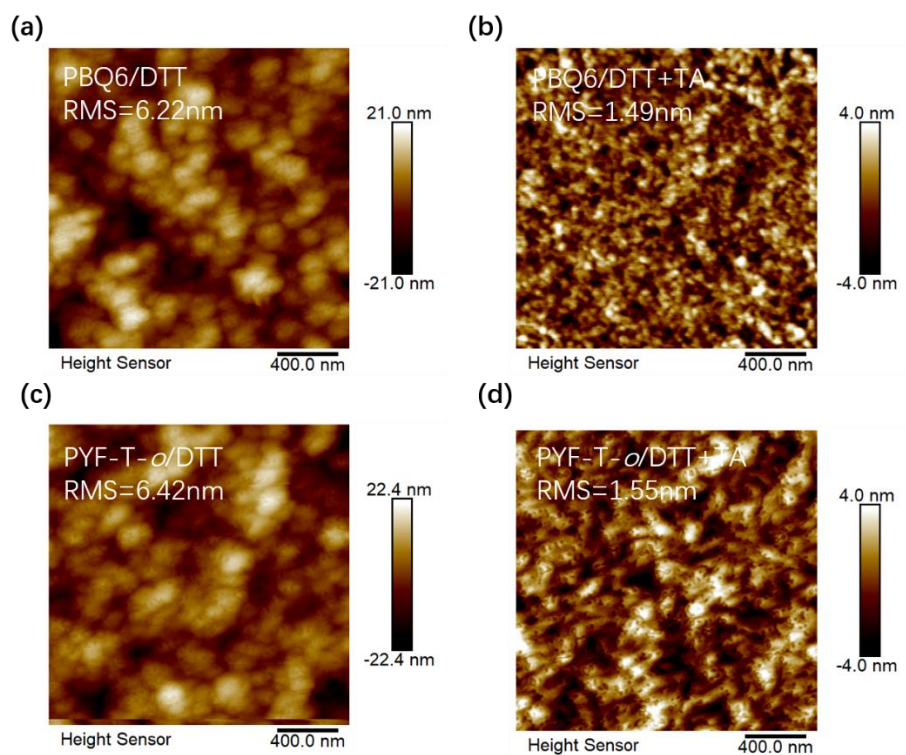


Figure S18. AFM surface scans of (a) PBQ6/DTT film without or (b) with TA at 90 °C for 10 min, and (c) PYF-T-*o*/DTT film without or (d) with TA at 90 °C for 10 min.

Supplementary Tables

Table S1. Photovoltaic performance parameters of the all-PSCs based on PBQ6:PYF-T-*o* (1:1, w/w, thermal annealing at 90°C for 10 min) with different additives under the illumination of AM 1.5G, 100 mW cm⁻².

Active layer	Additive	V_{oc} (V)	J_{sc} (mA cm ⁻²)	FF (%)	PCE (%)
PBQ6:PYF-T- <i>o</i>	CN	0.890	23.62	73.01	15.35
	DIO	0.872	24.24	65.36	13.82
	DTT	0.886	25.12	76.64	17.06
	DIB	0.887	22.46	60.54	12.06
	1-MN	0.896	22.12	72.08	14.29

Table S2. Photovoltaic performance parameters of the all-PSCs based on PBQ6:PYF-T-*o* (1:1, w/w, thermal annealing at 90°C for 10 min) with different solvents (with 275% DTT) under the illumination of AM 1.5G, 100 mW cm⁻².

Solvent	V_{oc} (V)	J_{sc} (mA cm ⁻²)	FF (%)	PCE (%)
<i>o</i> -xylene	0.886	23.25	72.63	14.96
toluene	0.886	25.12	76.64	17.06
THF	0.887	23.65	71.54	15.01
1,2,4-TMB	0.882	22.54	71.31	14.18
CF	0.886	24.50	77.02	16.72

Table S3. Photovoltaic performance parameters of the all-PSCs based on PBQ6:PYF-T-*o*/DTT with different weight ratios (thermal annealing at 90°C for 10 min) under the illumination of AM 1.5G, 100 mW cm⁻².

Active layer	D/A weight ratio	V_{oc} (V)	J_{sc} (mA cm ⁻²)	FF (%)	PCE (%)
PBQ6:PYF-T- <i>o</i>	0.7:1	0.883	24.45	73.94	15.96
	1:1	0.886	25.12	76.64	17.06
	1:1.3	0.885	24.66	74.17	16.13

Table S4. Photovoltaic performance parameters of the all-PSCs based on PBQ6:PYF-T-*o* (1:1, w/w, thermal annealing at 90°C for 10 min) with different weight ratio of DTT solid additive treatment under the illumination of AM 1.5G, 100 mW cm⁻².

weight ratio of DTT (%)	V_{oc} (V)	J_{sc} (mA cm ⁻²)	FF (%)	PCE (%)
200	0.886	24.02	72.67	15.47
225	0.884	24.42	73.38	15.84
250	0.885	24.95	75.04	16.57
275	0.886	25.12	76.64	17.06
300	0.887	24.63	76.45	16.70
350	0.886	24.38	75.52	16.31
400	0.888	23.82	76.06	16.09
500	0.885	23.65	75.62	15.83

Table S5. Effect of PBQ6 molecular weight on the photovoltaic performance of the all-PSCs based on PBQ6: PYF-T-*o*, under the illumination of AM1.5G, 100 mW cm⁻².

M_n (kDa) of PBQ6	V_{oc} (V)	J_{sc} (mA cm ⁻²)	FF (%)	PCE (%)
8.8	0.897	23.50	73.27	15.44
28.7	0.886	25.12	76.64	17.06
38.1	0.876	24.56	74.12	15.95

Table S6. Summary of photovoltaic performance parameters of the all-PSCs processed with halogenated solvent.

Active layer	V_{oc} (V)	J_{sc} (mA cm ⁻²)	FF (%)	PCE (%)	Ref.
PTzBI-Si:N2200	0.86	15.8	73	10.0	1
PM6:PZ1	0.96	17.1	68.2	11.2	2
PM6:PYT	0.93	21.78	66.33	13.44	3
PBDB-T:PTPBT-ET _{0.3}	0.899	21.33	65.3	12.53	4
PM6:L14	0.96	20.6	72.1	14.3	5
PBDB-T:PF5-Y5	0.946	20.65	74.0	14.45	6
PM6:PY-IT	0.933	22.30	72.3	15.05	7
PTzBI- <i>o</i> F:PFA1	0.87	23.96	72.67	15.11	8
PBDB-T:PJ1	0.90	22.7	75.3	15.4	9
PBDB-T:PZT- γ	0.896	24.7	71.3	15.8	10
JD40:PJ1	0.91	23.2	75	15.8	11
PBDB-T:PYT	0.891	23.03	73.98	15.17	12
PM6:PY-IT	0.937	21.90	73.6	15.11	13
PM6:PY-DT	0.949	23.73	74.4	16.67	14
PM6:L15:MBTI	0.957	22.91	73.83	16.18	15
PM6:PY-IT:N2200	0.947	22.60	74.9	16.04	16

PM6:PYT:PY2F-T	0.90	25.2	76	17.2	17
PM6:PTQ10:PY-IT	0.94	23.79	75.2	16.52	18
J71:N2200	0.910	13.12	78	9.31	19
PM6:PN1	1.00	15.2	69	10.5	20
PBDB-T:BSS10	0.86	18.55	64	10.1	21
PM6:PFBDT-IDTIC	0.96	15.27	68	10.3	22
PTzBI-Si:N2200	0.85	17.2	77.9	11.5	23
PBDTTT-E-T: DCNBT-TPIC	0.70	22.52	64.8	10.22	24
PM6:PF3-DTCO	0.943	15.75	68.2	10.13	25
PM6:PF2-DTSi	0.99	16.48	66.1	10.77	26
PBDB-T:PJ1	0.90	22.6	71	14.4	27
CD1:PBN-12	1.17	13.39	64	10.07	28
PBDB-T:PN-Sc	0.907	24.82	71.8	16.16	29
PM6:PY-IT:PYCl-T	0.920	24.64	73.31	16.62	30
PTzBI-oF:PM6:PFA1	0.880	24.36	76.14	16.3	31
PBQ6:PYF-T-o	0.886	25.12	76.64	17.06	This Work

Table S7. Summary of photovoltaic performance parameters of representative all-PSCs processed by various non-halogenated solvents.

Active layer	Solvents	V_{oc} (V)	J_{sc} (mA cm ⁻²)	FF (%)	PCE (%)	Ref.
HFAQx-T:N2200	THF	0.92	12.47	65	7.45	32
PBDT-TS1:PPDIODT	Anisole	0.76	15.72	55.11	6.58	33
PiI-2T-PS10:P(TP)	Toluene	0.98	9.93	51	5.10	34
PBDT-TS1:PPDIODT	<i>o</i> -MA	0.74	13.77	52.46	5.6	35
PTB7-Th:PDI-V	THF	0.74	15.5	70	8.1	36
PTzBI:N2200 _{HW}	2-MeTHF	0.849	15.17	70.36	9.16	37
PTzBI-Si:N2200	2-MeTHF	0.865	73.76	15.76	10.1	38
PTzBI-Si:N2200	CPME	0.85	77.9	16.5	11.0	39

PTzBI-Si:N2200	2-MeTHF	0.88	75.78	17.62	11.76	40
J51:PTB7-Th:N2200	CPME	0.82	67.8	17.27	9.6	41
PBDT5-TPD ₄ :P(NDI2HD-T)	2-MeTHF	1.02	55.75	14.42	8.2	42
PTzBI-Si:N2200	CPME	0.87	72.7	14.6	9.3	43
PTzBI-oF:PS1	2-MeTHF	0.92	66.70	22.47	13.8	44
PBDB-T:PJ1:PJ2	<i>o</i> -XY	0.91	72.98	21.46	14.28	45
PM6:L14	<i>o</i> -XY	0.953	74.10	22.10	15.62	46
PBQ6:PYF-T- <i>o</i>	Toluene	0.886	25.12	76.64	17.06	This Work

Table S8. The charge carriers mobilities of devices with thermal annealing at 90°C for 5 minutes.

blend	μ_e	μ_h	μ_h/μ_e
	[*10 ⁻⁴ cm ² V ⁻¹ s ⁻¹]	[*10 ⁻⁴ cm ² V ⁻¹ s ⁻¹]	
PBQ6:PYF-T- <i>o</i> /CN	7.33	4.44	0.607
PBQ6:PYF-T- <i>o</i> /DTT	8.41	6.19	0.736

The mobilities are average values measured from 6 devices.

Table S9. GIWAXS test performance parameters of the related neat and blend films.

	π - π stacking distance (010)		π - π stacking coherence (010)	
	Location	<i>d</i> -spacing	FWHM	CCL
	(Å ⁻¹)	(Å)	(Å ⁻¹)	(Å)
PBQ6	1.68	3.74	0.24	23.6
PBQ6/CN	1.70	3.69	0.23	24.4
PBQ6/DTT	1.71	3.68	0.21	27.1
PYF-T- <i>o</i>	1.60	3.94	0.31	18.6
PYF-T- <i>o</i> /CN	1.59	3.96	0.29	19.7
PYF-T- <i>o</i> /DTT	1.60	3.93	0.29	19.9
PBQ6:PYF-T- <i>o</i> /CN	1.68	3.74	0.23	25.3

PBQ6:PYF-T- <i>o</i> /DTT	1.69	3.73	0.21	26.8
---------------------------	------	------	------	------

Table S10. Summary of the domain size and domain purity

blend	Peak 1	Log period	ISI 1	Peak 2	Log period	ISI 2
	(nm ⁻¹)	(nm)		(nm ⁻¹)	(nm)	
PBQ6:PYF-T- <i>o</i> /CN	0.058	108	5.0 e ⁻²³	0.165	38	4.4 e ⁻²³
PBQ6:PYF-T- <i>o</i> /DTT	0.085	74	8.7 e ⁻²³	0.183	34	6.0 e ⁻²³

References

1. K. Zhang, R. Xia, B. Fan, X. Liu, Z. Wang, S. Dong, H. L. Yip, L. Ying, F. Huang and Y. Cao, *Adv. Mater.*, 2018, **30**, 1803166.
2. Y. Meng, J. Wu, X. Guo, W. Su, L. Zhu, J. Fang, Z.-G. Zhang, F. Liu, M. Zhang, T. P. Russell and Y. Li, *Sci. China Chem.*, 2019, **62**, 845-850.
3. W. Wang, Q. Wu, R. Sun, J. Guo, Y. Wu, M. Shi, W. Yang, H. Li and J. Min, *Joule*, 2020, **4**, 1070-1086.
4. J. Du, K. Hu, L. Meng, I. Angunawela, J. Zhang, S. Qin, A. Liebman-Pelaez, C. Zhu, Z. Zhang, H. Ade and Y. Li, *Angew. Chem., Int. Ed. Engl.*, 2020, **59**, 15181-15185.
5. H. Sun, H. Yu, Y. Shi, J. Yu, Z. Peng, X. Zhang, B. Liu, J. Wang, R. Singh, J. Lee, Y. Li, Z. Wei, Q. Liao, Z. Kan, L. Ye, H. Yan, F. Gao and X. Guo, *Adv. Mater.*, 2020, **32**, 2004183.
6. Q. Fan, Q. An, Y. Lin, Y. Xia, Q. Li, M. Zhang, W. Su, W. Peng, C. Zhang, F. Liu, L. Hou, W. Zhu, D. Yu, M. Xiao, E. Moons, F. Zhang, T. D. Anthopoulos, O. Inganäs and E. Wang, *Energy Environ. Sci.*, 2020, **13**, 5017-5027.
7. Z. Luo, T. Liu, R. Ma, Y. Xiao, L. Zhan, G. Zhang, H. Sun, F. Ni, G. Chai, J. Wang, C. Zhong, Y. Zou, X. Guo, X. Lu, H. Chen, H. Yan and C. Yang, *Adv. Mater.*, 2020, **32**, 2005942.
8. F. Peng, K. An, W. Zhong, Z. Li, L. Ying, N. Li, Z. Huang, C. Zhu, B. Fan, F.

- Huang and Y. Cao, *ACS Energy Lett.*, 2020, **5**, 3702-3707.
9. L. Zhang, T. Jia, L. Pan, B. Wu, Z. Wang, K. Gao, F. Liu, C. Duan, F. Huang and Y. Cao, *Sci. China Chem.*, 2021, **64**, 408-412.
 10. H. Fu, Y. Li, J. Yu, Z. Wu, Q. Fan, F. Lin, H. Y. Woo, F. Gao, Z. Zhu and A. K. Jen, *J. Am. Chem. Soc.*, 2021, **143**, 2665-2670.
 11. T. Jia, J. Zhang, K. Zhang, H. Tang, S. Dong, C.-H. Tan, X. Wang and F. Huang, *J. Mater. Chem. A*, 2021, **9**, 8975-8983.
 12. Q. Wu, W. Wang, Y. Wu, Z. Chen, J. Guo, R. Sun, J. Guo, Y. Yang and J. Min, *Adv. Funct. Mater.*, 2021, **31**, 2010411.
 13. T. Liu, T. Yang, R. Ma, L. Zhan, Z. Luo, G. Zhang, Y. Li, K. Gao, Y. Xiao, J. Yu, X. Zou, H. Sun, M. Zhang, T. A. Dela Peña, Z. Xing, H. Liu, X. Li, G. Li, J. Huang, C. Duan, K. S. Wong, X. Lu, X. Guo, F. Gao, H. Chen, F. Huang, Y. Li, Y. Li, Y. Cao, B. Tang and H. Yan, *Joule*, 2021, **5**, 914-930.
 14. Y. Li, J. Song, Y. Dong, H. Jin, J. Xin, S. Wang, Y. Cai, L. Jiang, W. Ma, Z. Tang and Y. Sun, *Adv. Mater.*, 2022, **34**, 2110155.
 15. H. Sun, B. Liu, Y. Ma, J. W. Lee, J. Yang, J. Wang, Y. Li, B. Li, K. Feng, Y. Shi, B. Zhang, D. Han, H. Meng, L. Niu, B. J. Kim, Q. Zheng and X. Guo, *Adv. Mater.*, 2021, **33**, e2102635.
 16. R. Ma, J. Yu, T. Liu, G. Zhang, Y. Xiao, Z. Luo, G. Chai, Y. Chen, Q. Fan, W. Su, G. Li, E. Wang, X. Lu, F. Gao, B. Tang and H. Yan, *Aggregate*, 2021, **3**.
 17. R. Sun, W. Wang, H. Yu, Z. Chen, X. Xia, H. Shen, J. Guo, M. Shi, Y. Zheng, Y. Wu, W. Yang, T. Wang, Q. Wu, Y. Yang, X. Lu, J. Xia, C. J. Brabec, H. Yan, Y. Li and J. Min, *Joule*, 2021, **5**, 1548-1565.
 18. W. Zhang, C. Sun, I. Angunawela, L. Meng, S. Qin, L. Zhou, S. Li, H. Zhuo, G. Yang, Z. G. Zhang, H. Ade and Y. Li, *Adv. Mater.*, 2022, **34**, 2108749.
 19. X. Liu, X. Li, N. Zheng, C. Gu, L. Wang, J. Fang and C. Yang, *ACS Appl. Mater. Interfaces*, 2019, **11**, 43433-43440.
 20. J. Wu, Y. Meng, X. Guo, L. Zhu, F. Liu and M. Zhang, *J. Mater. Chem. A*, 2019, **7**, 16190-16196.

21. N. B. Kolhe, D. K. Tran, H. Lee, D. Kuzuhara, N. Yoshimoto, T. Koganezawa and S. A. Jenekhe, *ACS Energy Lett.*, 2019, **4**, 1162-1170.
22. H. Yao, F. Bai, H. Hu, L. Arunagiri, J. Zhang, Y. Chen, H. Yu, S. Chen, T. Liu, J. Y. L. Lai, Y. Zou, H. Ade and H. Yan, *ACS Energy Lett.*, 2019, **4**, 417-422.
23. Z. Li, W. Zhong, L. Ying, F. Liu, N. Li, F. Huang and Y. Cao, *Nano Energy*, 2019, **64**, 103931.
24. J. H. K. Feng, X. Zhang, Z. Wu, S. Shi, L. Thomsen, Y. Tian, H. Y. Woo, C.R. McNeill and X. Guo, *Adv. Mater.*, 2020, **32**, 2070226.
25. Q. Fan, W. Su, S. Chen, T. Liu, W. Zhuang, R. Ma, X. Wen, Z. Yin, Z. Luo, X. Guo, L. Hou, K. Moth-Poulsen, Y. Li, Z. Zhang, C. Yang, D. Yu, H. Yan, M. Zhang and E. Wang, *Angew. Chem., Int. Ed. Engl.*, 2020, **59**, 19835-19840.
26. Q. Fan, W. Su, S. Chen, W. Kim, X. Chen, B. Lee, T. Liu, U. A. Méndez-Romero, R. Ma, T. Yang, W. Zhuang, Y. Li, Y. Li, T.-S. Kim, L. Hou, C. Yang, H. Yan, D. Yu and E. Wang, *Joule*, 2020, **4**, 658-672.
27. T. Jia, J. Zhang, W. Zhong, Y. Liang, K. Zhang, S. Dong, L. Ying, F. Liu, X. Wang, F. Huang and Y. Cao, *Nano Energy*, 2020, **72**, 104718.
28. R. Zhao, N. Wang, Y. Yu and J. Liu, *Chem. Mater.*, 2020, **32**, 1308-1314.
29. J. Du, K. Hu, J. Zhang, L. Meng, J. Yue, I. Angunawela, H. Yan, S. Qin, X. Kong, Z. Zhang, B. Guan, H. Ade and Y. Li, *Nat. Commun.*, 2021, **12**, 5264.
30. K. Hu, J. Du, C. Zhu, W. Lai, J. Li, J. Xin, W. Ma, Z. Zhang, J. Zhang, L. Meng and Y. Li, *Sci. China Chem.*, 2022, **65**, 954-963.
31. K. An, F. Peng, W. Zhong, W. Deng, D. Zhang, L. Ying, H. Wu, F. Huang and Y. Cao, *Sci. China Chem.*, 2021, **64**, 2010-2016.
32. L. Zhou, X. He, T. K. Lau, B. Qiu, T. Wang, X. Lu, B. Luszczynska, J. Ulanski, S. Xu, G. Chen, J. Yuan, Z. G. Zhang, Y. Li and Y. Zou, *ACS Appl. Mater. Interfaces*, 2018, **10**, 41318-41325.
33. S. Li, H. Zhang, W. Zhao, L. Ye, H. Yao, B. Yang, S. Zhang and J. Hou, *Adv. Energy Mater.*, 2016, **6**, 1501991.
34. Y. Zhou, K. L. Gu, X. Gu, T. Kurosawa, H. Yan, Y. Guo, G. I. Koleilat, D. Zhao,

- M. F. Toney and Z. Bao, *Chem. Mater.*, 2016, **28**, 5037-5042.
35. L. Ye, Y. Xiong, S. Li, M. Ghasemi, N. Balar, J. Turner, A. Gadisa, J. Hou, B. T. O'Connor and H. Ade, *Adv. Funct. Mater.*, 2017, **27**, 1702016.
36. Y.-k. G. W.-t. Xiong, D.-h. Zhao and Y.-m. Sun, *Acta Polym. Sin.*, 2018, **2**, 315-320.
37. B. Fan, L. Ying, Z. Wang, B. He, X.-F. Jiang, F. Huang and Y. Cao, *Energy Environ. Sci.*, 2017, **10**, 1243-1251.
38. B. Fan, L. Ying, P. Zhu, F. Pan, F. Liu, J. Chen, F. Huang and Y. Cao, *Adv. Mater.*, 2017, **29**, 1703906.
39. Z. Li, L. Ying, P. Zhu, W. Zhong, N. Li, F. Liu, F. Huang and Y. Cao, *Energy Environ. Sci.*, 2019, **12**, 157-163.
40. L. Zhu, W. Zhong, C. Qiu, B. Lyu, Z. Zhou, M. Zhang, J. Song, J. Xu, J. Wang, J. Ali, W. Feng, Z. Shi, X. Gu, L. Ying, Y. Zhang and F. Liu, *Adv. Mater.*, 2019, **31**, 1902899.
41. Q. Zhang, Z. Chen, W. Ma, Z. Xie, J. Liu, X. Yu and Y. Han, *ACS Appl. Mater. Interfaces*, 2019, **11**, 32200-32208.
42. W. Feng, Z. Lin, C. Lin, W. Wang and Q. Ling, *ACS Appl. Mater. Interfaces*, 2019, **11**, 43441-43451.
43. Z.-Y. Li, W.-K. Zhong, L. Ying, N. Li, F. Liu, F. Huang and Y. Cao, *Chin. J. Polym. Sci.*, 2019, **38**, 323-331.
44. C. Zhu, Z. Li, W. Zhong, F. Peng, Z. Zeng, L. Ying, F. Huang and Y. Cao, *Chem. Commun.*, 2021, **57**, 935-938.
45. J. Zhang, T. Jia, C.-H. Tan, K. Zhang, M. Ren, S. Dong, Q. Xu, F. Huang and Y. Cao, *Sol. RRL*, 2021, **5**, 2100076.
46. B. Liu, H. Sun, J.-W. Lee, J. Yang, J. Wang, Y. Li, B. Li, M. Xu, Q. Liao, W. Zhang, D. Han, L. Niu, H. Meng, B. J. Kim and X. Guo, *Energy Environ. Sci.*, 2021, **14**, 4499-4507.